LUND
UNIVERSITY

Bachelor Thesis

eulerr: Area-Proportional Euler Diagrams with Ellipses

Johan Larsson

supervised by
Peter Gustafsson

December 27, 2017

Submitted in partial fulfillment of the requirements for the degree of
Bachelor of Science in Statistics
at the Department of Statistics, Lund University

Contents

Abstract

Stuff

1 Background

Data visualizations represent one of the most intuitive forms of data presentation. Because they work on multiple dimensions, they possess the potential to convey intricate relationships that single statistics or tables never can.

Visualizations are most effective when they show relationships. Consider, for instance, a disc labelled *Men*[1]—it says nothing by itself; yet if we juxtapose it with another, smaller, disc labelled *Children*[2], the graphic starts to become informative, now displaying the relative sizes of two sets. If we moreover proceed to intersect the two discs, producing an overlap, we successfully visualize the relative proportions of men and children, as well as their intersection. The diagram we have constructed is an *Euler diagram*[3].

1

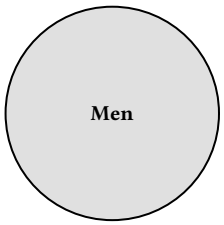

2

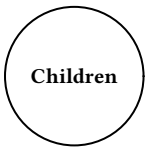

3

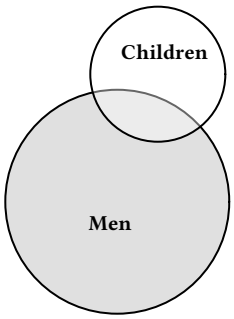

The Euler diagram, originally proposed by Leonard Euler [1], is a generalization of the obiquiteous *Venn diagram*, the latter being a staple of introductory text books in statistics and research disciplines such as biomedicine and geology. Venn and Euler diagrams both displays set relationships but differ in that the the former require all intersections to be present—even if they are empty—which Euler diagrams do not.

Euler diagrams may moreover be area-proportional, which is to say that each separate surface of the diagram maps to some quantity. (This is the case with the diagram to the right.) This is a rational form for a Euler diagram—only its geometries are necessary to interpret it. It lets us, for instance, to discard numbers without losing critical information; the same cannot be said for a Venn diagram.

Area-proportional Euler diagrams may be fashioned out of any closed shape, and have been implemented for triangles [2], rectangles [2], ellipses [3], smooth curves [4], polygons [2], and circles [2, 5, 6]. The latter is the popular choice, and for good reason, since they are easiest to interpret [7]. Yet, circles do not always support accurate diagrams. Consider the following three-set configuration:

$$A = B = C = 2,$$
$$A \cap B = A \cap C = B \cap C = 1, \text{ and}$$
$$A \cap B \cap C = 0.$$

There is no way to visualize this relationship perfectly with circles because they cannot be arranged to keep the $A \cap B \cap C$ overlap empty whilst $A \cap B$, $A \cap C$, and $B \cap C$ remain non-empty. With ellipses,

however, we can solve this problem since they can both rotate and stretch, enabling a perfect fit (Figure 1.1).

With four or more sets that all intersect, exact Euler diagrams are in fact impossible with circles, given that we *require* 15 intersections but with four circles can yield at most 13 unique overlaps. This is not the case with ellipses, which may intersect in up to four, rather than two, points, altogether yielding the necessary 15 unique areas. As of yet, the only implementation of elliptical Euler diagrams is provided in **eulerAPE** [3], although it only supports three sets that are all required to intersect. The diagram in Figure 1.2, for instance, would be impossible with **eulerAPE**.

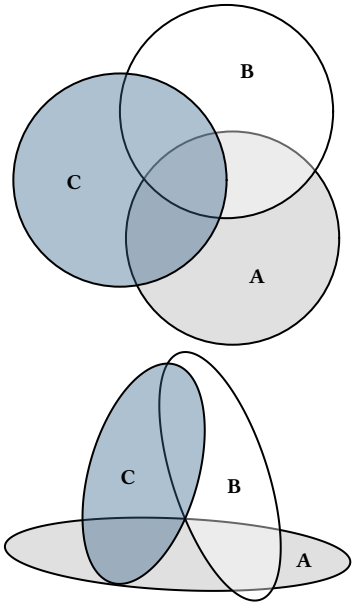

Figure 1.1. A set relationship depicted erroneously with circles and perfectly with ellipses.

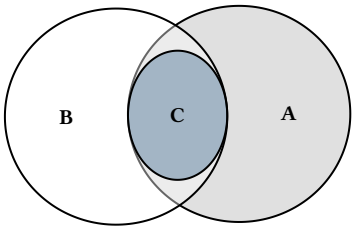

Figure 1.2. An Euler diagram with a subset relationship.

Euler diagrams have to be solved numerically [8]. Most software accomplish this in two steps, first finding a coarse starting layout that is finalized in a second, more thorough, algorithm. For the initial layout, the aforementioned **eulerAPE** package [9], for instance, uses a greedy algorithm that tries to minimize the error in the three-way intersection by arranging the circles representing the sets. The **venneuler** package [5], meanwhile, uses multidimensional scaling (MDS) with Jacobian distances, taking only pairwise relationships into account. **venn.js** [10] combines a constrained version of the MDS algorithm from **venneuler**, that is contrastingly based on euclidean distances, with a greedy algorithm, picking the best fit out of the two. **Vennerable** [2] computes the required pairwise distances between circles and then adjusts the largest of these to optimize the two-way overlaps of the layout. All of the above use circles in the initial layout.

Diagrams with more than two sets normally require additional tuning, the prerequisite for which is that we first know the areas of the overlaps so that we can assess how well our diagram fits the input. Computing overlaps, however, is no trivial task, particularly not for ellipses. This is evident in that many methods resort to approximations such as quadtrees [5] (**venneuler**) or polygon intersections [6] (**VennMaster**).

Compared to the approximative algorithms, exact algorithms require that we know the intersection points of the ellipses. There are two known approaches to this. Both treat the ellipses in pairs. The first method [11] solves the system of equations formed by each pair of ellipses, which involves solving a fourth-degree polynomial; the other method [12] represents the ellipses as conics in projective geometry, which reduces to solving a third-degree polynomial. Both methods are accurate up to floating-point precision.

With all the intersection points at hand, it is possible to derive the areas of the overlaps. Frederickson [10] (**venn.js**) and Micallef and Rodgers [3] (**eulerAPE**) has developed solutions for circles and ellipses respectively—although the latter, as we previously noted, is restricted to three intersecting ellipses. No algorithm has so far been published that extends these methods to any number

of ellipses or elliptical three-set diagrams with subset of disjoint intersections.

In the final layout, the package's area-algorithm is used with a numerical optimizer to tune the parameters of the diagram. All previously considered packages treat this as a minimization problem but their loss functions vary. **venn.js** uses the residual sums of squares[4], **venneuler** uses the *stress* metric[5], which is computed as the residual sums of squares over total sums of squares, **Vennerable** uses Chow's [13] idealistic function[6], and **eulerAPE** uses a proportional loss function[7] that severely punishes missing overlaps—in fact, it becomes undefined if such areas exist, making it inappropriate for algorithms that aims to fit set configurations with either subset or disjoint relationships.

venn.js relies on a Nelder–Mead optimizer for the final optimization. **venneuler**, on the other hand, runs a combination of steepest descent optimizer with gradient approximation and coordinate descent. **eulerAPE** and **Vennerable**, meanwhile, uses a hill climbing algorithm.

1.1 Aims

In this thesis, we aim to present an algorithm and software implementation for constructing and visualizing Euler diagrams for set relationships of any size using ellipses.

[4] **venn.js**'s loss function is

$$\sum_{i=1}^{n} (A_i - \omega_i)^2 ,$$

where n is the number of overlaps, ω_i the size of the i:th intersection and its relative complement, and A_i the corresponding overlap's area in the diagram.

[5] **venneuler**'s stress metric is defined as

$$\frac{\sum_{i=1}^{n}(A_i - \beta\omega_i)^2}{\sum_{i=1}^{n} A_i^2},$$

where $\beta = \frac{\sum_{i=1}^{n} A_i\omega_i}{\sum_{i=1}^{n} \omega_i^2}$.

[6] This idealistic function (used in **Vennerable**) is defined as

$$\sum_{i=1}^{n}\left(\frac{\omega_i}{\sum_{i=1}^{n}\omega_i} - \frac{A_i}{\sum_{i=1}^{n} A_i}\right)^2 + \sum_{i<j<n}\left(A_i - A_j\right),$$

where the sets and their respective overlaps corresponding to the indices i and j have been ordered so that $i < j \implies \omega_i < \omega_j$.

[7] **eulerAPE**'s cost function is defined as

$$\frac{1}{n}\sum_{i=1}^{n}\frac{(\omega_i - A_i)^2}{A_i}.$$

2 Method

Constructing an Euler diagram is much like fitting a statistical model in that we have

1. data,
2. a model—in this case a diagram—to fit the data with,
3. tests to assess the model's fit, and
4. a presentation of the result.

In the following sections, we explain how **eulerr** tackles each item in turn.

2.1 Input

Euler diagrams present relationships between sets, wherefore the data must describe these relationships, either directly or indirectly. **eulerr** allows several alternatives for this data, namely,

- intersections and relative complements[8],
- unions and identities[9],
- a matrix of binary (or boolean) indices[10],
- a list of sample spaces[11], or
- a two- or three-way table[12].

As an additional feature for the matrix form, the user may supply a factor variable with which to split the data set before fitting the diagram, which sometimes improves diagrams where the set relationships vary across categories.

Whichever type of input is provided, **eulerr** translates it to the first, *intersections and relative complements* (Definition 2.1), which is the form used later in the loss functions of the initial and final optimizers.

[8] $A \setminus B = 3 \quad B \setminus A = 2 \quad A \cap B = 1$

[9] $A = 4 \quad B = 3 \quad A \cap B = 1$

[10]
$$\begin{bmatrix} \boldsymbol{A} & \boldsymbol{B} \\ 1 & 0 \\ 1 & 0 \\ 1 & 0 \\ 1 & 1 \\ 0 & 1 \\ 0 & 1 \end{bmatrix}$$

[11] $A = \{a, b, c, d\}$
$B = \{a, e, f\}$

[12]

	A	A^c
B	1	2
B^c	3	0

Definition 2.1. *For a family of* N *sets,* $F = F_1, F_2, \ldots, F_N$*, and their* $n = 2^N - 1$ *intersections, we define* ω *as the intersections of these sets and their relative complements, such that*

$$\begin{aligned}
\omega_1 &= F_1 \setminus \bigcap_{i=2}^{N} F_i \\
\omega_2 &= \bigcap_{i=1}^{2} F_i \setminus \bigcap_{i=3}^{N} F_i \\
&\vdots \\
\omega_n &= \bigcap_{i=1}^{N} F_i
\end{aligned}$$

with

$$\sum_{i=1}^{n} \omega_i = \bigcup_{j=1}^{N} F_i.$$

Analogously to ω*, we also introduce the* & *operator, such that*

$$F_i \& F_j = (F_i \cap F_j) \setminus (F_i \cap F_j)^c = \omega_k,$$

where k *is the index of the* k^{th} *intersection between* F_i *and* F_j*.*

With the input translated into our form of choice, the Euler diagram is fit in two steps: first, an initial configuration is formed with circles using only the sets' pairwise relationships. Second, this configuration is fine tuned taking all $2^N - 1$ intersections into account.

2.2 Initial layout

For our initial layout, we employ a constrained version of multidimensional scaling (MDS) that has been adapted from **venn.js** [10], which in turn is a modification of an algorithm used in **venneuler** [5]. In it, we consider the pairwise relationships between the sets, attempting to position their respective shapes so as to minimize the difference between the separation between their centers required to obtain an optimal overlap (ω) and the actual overlap of the shapes in the diagram.

This problem is unfortunately intractable for ellipses, being that there is an infinite number of ways by which we can position two ellipses to obtain a given overlap. Thus, we restrict ourselves to circles in our initial layout, for which we can use the circle–circle overlap formula (2.1) to numerically find the required distance, d, for each pairwise relationship.

$$O_{ij} = r_i^2 \arccos\left(\frac{d_{ij}^2 + r_i^2 - r_j^2}{2 d_{ij} r_i}\right) + r_j^2 \arccos\left(\frac{d_{ij}^2 + r_j^2 - r_i^2}{2 d_{ij} r_j}\right) - \frac{1}{2}\sqrt{(-d_{ij} + r_i + r_j)(d_{ij} + r_i - r_j)(d_{ij} - r_i + r_j)(d_{ij} + r_i + r_j)}, \quad (2.1)$$

where r_i and r_j are the radii of the circles representing the i^{th} and j^{th} sets respectively, O_{ij} their overlap, and d_{ij} their separation.

Setting $r_i = \sqrt{\omega_i / \pi}$, where ω_i is the size of the i^{th} set, we are able to obtain d numerically using the squared difference between O and ω (the desired overlap), as loss function (2.2).

$$\mathcal{L}(d_{ij}) = (O_{ij} - \omega_{ij})^2, \quad \text{for } i < j \leq n, \tag{2.2}$$

which we optimize using `optimize()`[13] from **stats**.

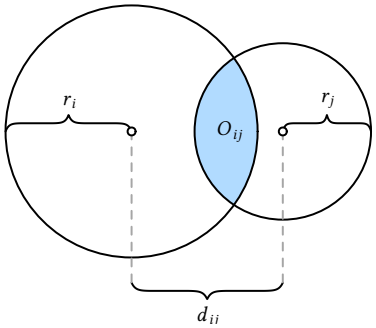

Figure 2.1. The circle–circle overlap is computed as a function of the discs' separation (d_{ij}), radii (r_i, r_j), and area of overlap (O_{ij}).

[13] According to the documentation, `optimize()` consists of a "combination of golden section search and successive parabolic interpolation."

For a two-set combination, this is all we need to plot an exact diagram, given that we now have the two circles' radii and separation and may place the circles arbitrarily as long as their separation, d, remains the same. This is not, however, the case with more than two sets.

With three or more sets, the circles need to be arranged so that they interfere minimally with one another. In some cases, the set configuration allows this to be accomplished flawlessly, but often, compromises must me made. As with many of the problems in this thesis, this turns out to be another optimization problem. It can be tackled in many ways; **eulerr**'s approach is based on a method developed by Frederickson [14], which the author describes as constrained multi-dimensional scaling.

The algorithm tries to position the circles so that the separation between each pair of circles matches the separation required from (2.2). If the two sets are disjoint, however, the algorithm is indifferent to the relative locations of those circles as long as they do not intersect. The equivalent applies to subset sets: as long as the circle representing the smaller set remains within the larger circle, their locations are free to vary. In all other cases, the loss function (2.3) is the residual sums of squares of the optimal separation of sets, d, that we found in (2.1), and the actual distance in the layout we are currently exploring.

$$\mathcal{L}(h, k) = \sum_{1 \leq i < j \leq N} \begin{cases} 0 & F_i \cap F_j = \emptyset \text{ and } O_{ij} = \emptyset \\ 0 & (F_i \subseteq F_j \text{ or } F_i \supseteq F_j) \text{ and } O_{ij} = \emptyset \\ \left(\left(h_i - h_j\right)^2 + \left(k_i - k_j\right)^2 - d_{ij}^2 \right)^2 & \text{otherwise} \end{cases}. \tag{2.3}$$

The analytical gradient (2.4) is retrieved as usual by taking the derivative of the loss function:

$$\vec{\nabla} f(h_i) = \sum_{j=1}^{N} \begin{cases} \vec{0} & F_i \cap F_j = \emptyset \text{ and } O_{ij} = \emptyset \\ \vec{0} & (F_i \subseteq F_j \text{ or } F_i \supseteq F_j) \text{ and } O_{ij} = \emptyset \\ 4\left(h_i - h_j\right) \left(\left(h_i - h_j\right)^2 + \left(k_i - k_j\right)^2 - d_{ij}^2 \right) & \text{otherwise,} \end{cases} \tag{2.4}$$

where $\vec{\nabla} f(k_i)$ is found as in (2.4) with h_i swapped for k_i (and vice versa).

The Hessian (2.5) for our loss function is given next. However, because the current release of R suffers from a bug that causes the analytical Hessian to be updated improperly, the current release of **eulerr** instead relies on the numerical approximation of the Hessian offered by the optimizer[14].

$$\boldsymbol{H} = \sum_{1 \leq i < j \leq N} \begin{bmatrix} 4\left(\left(h_i - h_j\right)^2 + \left(k_i - k_j\right)^2 - d_{ij}^2\right) + 8\left(h_i - h_j\right)^2 & \cdots & 8\left(h_i - h_j\right)\left(k_i - k_j\right) \\ \vdots & \ddots & \vdots \\ 8\left(k_i - k_j\right)\left(h_i - h_j\right) & \cdots & 4\left(\left(h_i - h_j\right)^2 + \left(k_i - k_j\right)^2 - d_{ij}^2\right) + 8\left(k_i - k_j\right)^2 \end{bmatrix}. \tag{2.5}$$

Note that the constraints given in (2.3) and (2.4) still apply to each element of (2.5) and have been omitted for convenience only.

We optimize (2.3) using the nonlinear optimizer `nlm()` from the R core package **stats**. The underlying code for `nlm()` was written by Schnabel et al. [15]. It was ported to R by Saikat DebRoy and the R Core team [16] from a previous FORTRAN to C translation by Richard H. Jones. `nlm()` consists of a system of Newton-type algorithms and performs well for difficult problems [17].

The initial layout outlined above will sometimes turn up perfect diagrams, but only reliably so when the diagram is completely determined by its pairwise intersections. More pertinently, we have not yet considered the higher-order intersections in our algorithm and neither have we approached the problem of using ellipses—as we set out to do.

[14] The current development version of R features a fix for this bug; it is our intent to switch to using the analytical Hessian as soon as it is introduced in a stable version of R.

2.3 Final layout

We now need to account for all the sets' relationships and, consequently, all the overlaps in the diagram. We initially restricted ourselves to circles but now extend ourselves also to ellipses. From now on, we abandon the practice of treating circles separately—they are only a special case of ellipses, and, hence, everything that applies to an ellipse does so equally for a circle.

2.3.1 Intersecting ellipses

As we briefly discussed in chapter 1, we now need the ellipses' points of intersections. **eulerr**'s approach to this is outlined in Richter-Gebert [12] and based in *projective*, as opposed to *euclidean*, geometry.

To collect all the intersection points, we naturally need only to consider two ellipses at a time. The canonical form of an ellipse is given by

$$\frac{\left[(x-h)\cos\phi + (y-k)\sin\phi\right]^2}{a^2} + \frac{\left[(x-h)\sin\phi - (y-k)\cos\phi\right]^2}{b^2} = 1,$$

where ϕ is the counter-clockwise angle from the positive x-axis to the semi-major axis a, b is the semi-minor axis, and h, k are the x- and y-coordinates, respectively, of ellipse's center. However, because an ellipse is a conic[15] it can be represented in quadric form,

$$Ax^2 + Bxy + Cy^2 + Dx + Ey + F = 0$$

that in turn can be represented as a matrix,

$$\begin{bmatrix} A & B/2 & D/2 \\ B/2 & C & E/2 \\ D/2 & E/2 & F \end{bmatrix},$$

which is the form we need to intersect our ellipses. We now proceed to

1. form three degenerate conics from a linear combination of the two ellipses we wish to intersect,
2. split one of these degenerate conics into two lines, and
3. intersect one of the ellipses with these lines, yielding 0 to 4 intersection points points (Figure 2.2).

[15] The circle, parabola, and hyperbola are the other types of conics.

2.3.2 Computing the areas of the intersections

Using the intersection points of a set of ellipses that we retrieved in subsection 2.3.1, we can now find the overlap of these ellipses. We are only interested in the points that are *contained within all of these ellipses*, which together form a geometric shape consisting of a convex polygon, the sides of which are made up of straight lines between consecutive points, and a set of elliptical arcs—one for each pair of points (Figure 2.3).

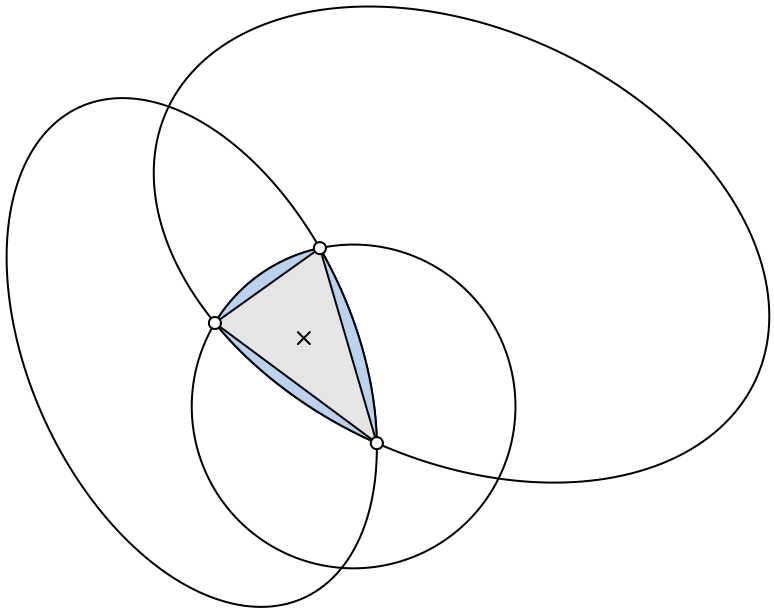

Figure 2.3. The overlap area between three ellipses is the sum of a convex polygon (in grey) and 2–3 ellipse segments (in blue).

We continue by ordering the points around their centroid. It is then trivial to find the area of the polygon section since it is always convex [18]. Now, because each elliptical segment is formed from the arcs that connect successive points, we can establish the segments' areas algorithmically [11]. For each ellipse and its related pair of points (located at angles θ_0 and θ_1 from the semimajor axis), we proceed to find its area by

1. centering the ellipse at $(0, 0)$,
2. normalizing its rotation, which is not needed to compute the area,
3. integrating the ellipse in $[0, \theta_0]$ and $[0, \theta_1]$, producing elliptical sectors $F(\theta_0)$ and $F(\theta_1)$,
4. subtracting the smaller ($F(\theta_0)$) of these sectors from the larger ($F(\theta_0)$, and
5. subtracting the triangle section to finally find the segment area,

$$F(\theta_1) - F(\theta_0) - \frac{1}{2}\left|x_1 y_0 - x_0 y_1\right|,$$

$$\text{where } F(\theta) = \frac{a}{b}\left[\theta - \arctan\left(\frac{(b-a)\sin 2\theta}{b + a + (b-a)\cos 2\theta}\right)\right].$$

This procedure is illustrated in Figure 2.4. Note that there are situations where this algorithm is altered, such that when the sector angle ranges beyond π—we refer the interested reader to Eberly [11].

Finally, the area of the overlap is then obtained by adding the area of the polygon and all the elliptical arcs together.

Note that this does not yet give us the areas that we require, namely the area-equivalents to the set intersections and relative complements from Definition 2.1. For this, we must also decompose the overlap areas hierarchically, so that each area maps uniquely to a subspace of the set configuration. This, however, is simply a matter of transversing down the hierarchy of overlaps and subtracting the higher-order overlaps from the lower-order ones. For a three-set relationship of sets A, B, and C, for instance, this means subtracting the $A \cap B \cap C$ overlap from the $A \cap B$ one to retrieve the equivalent of $(A \cap B) \setminus C$.

The exact algorithm may in rare instances[16], break down, the culprit being numerical precision issues that occur when ellipses are tangent or completely overlap. In these cases, the algorithm will approximate the area of the involved overlap by

1. spreading points across the ellipses using Vogel's method (see section A.1 for a brief introduction),

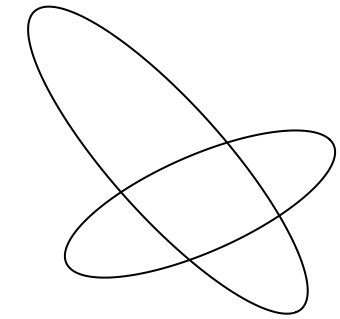

(a) Our objective is two intersect these two ellipses.

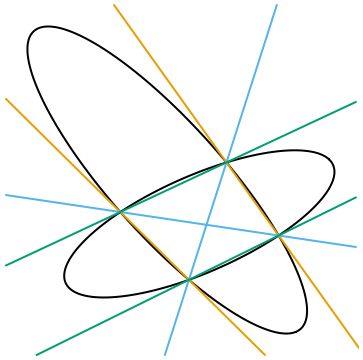

(b) Three degenerate conics (orange, teal, and blue) are formed from the linear combination of our two ellipses.

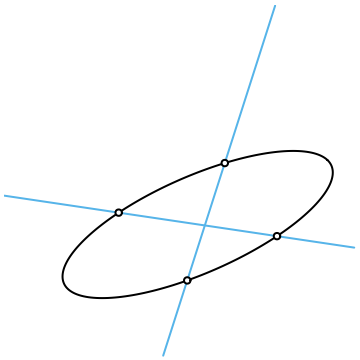

(c) One of the degenerate conics is split it into two lines and intersected with one of the ellipses to yield four intersection points.

Figure 2.2. The process used to intersect two ellipses, here yielding four points. This figure was inspired by an example from Richter-Gebert [12].

2. identifying the points that are inside the intersection via the inequality

$$\frac{[(x-h)\cos\phi + (y-k)\sin\phi]^2}{a^2} + \frac{[(x-h)\sin\phi - (y-k)\cos\phi]^2}{b^2} < 1,$$

where x and y are the coordinates of the sampled points, and finally

3. approximating the area by multiplying the proportion of points inside the overlap with the area of the ellipse.

With this in place, we are now able to compute the areas of all intersections and their relative complements up to numerical precision.

We feed the initial layout computed in section 2.2 to the optimizer—once again we employ `nlm()` from **stats** but now also provide the option to use ellipses rather than circles, allowing the "circles" to rotate and the relation between the semiaxes to vary, altogether rendering five parameters to optimize per set and ellipse (or three if we restrict ourselves to circles). For each iteration of the optimizer, the areas of all intersections are analyzed and a measure of loss returned. The loss we use is the same as that in **venneuler** [5], namely *stress*,

$$\frac{\sum_{i=1}^{n}(A_i - \beta\omega_i)^2}{\sum_{i=1}^{n} A_i}, \tag{2.6}$$

where

$$\beta = \frac{\sum_{i=1}^{n} A_i\omega_i}{\sum_{i=1}^{n} \omega_i^2}.$$

This is the equivalent of fitting a linear regression through the origin, where β is the slope of the regression line (Figure 2.5).

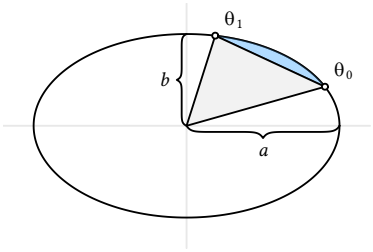

Figure 2.4. The elliptical segment in blue is found by first subtracting the elliptical sector from $(a, 0)$ to θ_0 from the one from $(a, 0)$ to θ_1 and then subtracting the triangle part (in grey).

[16] 1 out of approximately 7000 in our simulations.

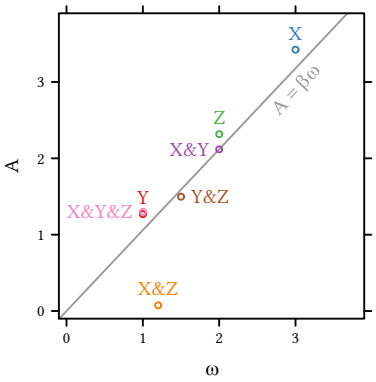

Figure 2.5. Optimizing via stress is akin to fitting a least-squares linear regression through the origin.

[17] We conducted thorough benchmarking, that we opt not to report here, to decide upon an algorithm for this step.

[18] The choice of if and when this last-ditch optimizer is activated is left to the user via simple commands to the main function of the package.

2.3.3 Last-ditch optimization

If we are using ellipses and are faced with an error in our fit, we offer a final step in which we pass the parameters on to a last-ditch optimizer. The weapon of choice[17] is a *differential evolution algorithm* from the R package **RcppDE** [19]—a port of the **DEoptim** package [20] from C to C++.

The solutions offered by **RcppDE** often avoid local minimi but may be inefficient in local search regions; this shortcoming can be remedied by fine tuning with a local optimizer [21]—once more, we rely on `nlm()` to serve this purpose.

By default, this last-ditch step is activated only when we have a three-set diagram with ellipses and a diagError (2.7) above 0.001[18] The reason being that the method is considerably more computationally intensive.

2.4 Goodness of fit

When **eulerr** cannot find a perfect solution, it offers an approximate one instead, the adequacy of which has to be measured in a standardized way. For this purpose we adopt two measures: *stress* [5], which is also the loss metric we use in our final optimization step and is used in **venneuler**, as well as *diagError* [3], which is used by **eulerAPE**.

We first encountered the stress metric (2.6) in chapter 1 and covered it again in section 2.3. The stress metric is not easily grasped but can be transformed into a rough analogue of the correlation coefficient via $r = \sqrt{1 - \text{stress}^2}$.

diagError, meanwhile, is given by

$$\max_{i=1,2,\ldots,n} \left| \frac{\omega_i}{\sum_{i=1}^{n} \omega_i} - \frac{A_i}{\sum_{i=1}^{n} A_i} \right|, \tag{2.7}$$

which is the maximum *absolute* difference of the proportion of any ω to the respective unique area of the diagram.

3 Results

The only R packages that feature area-proportional Euler diagrams are **eulerr**, **venneuler**, **Vennerable**, and **d3VennR**. The latter is an interface to the **venn.js** script that has been discussed previously, but because it features an outdated version of the script and only produces images as html, we call **venn.js** directly using the javascript engine **V8** via the R package of the same name [22]. Only **eulerr**, **venn.js**, and **venneuler** support more than three sets, which is why there are only three-set results for **Vennerable** and **eulerAPE**.

The packages used here were

- **eulerr** 3.1.0,
- **eulerAPE** 3.0.0,
- **venn.js** 0.2.14,
- **venneuler** 1.1-0, and
- **Vennerable** 3.1.0.9000.

The results for **eulerAPE** were computed on a laptop computer[19]. The remaining results were computed on an Amazon EC2 cloud-based computing instance[20].

3.1 Case studies

We begin our examination of **eulerr** by studying a difficult set relationship from Wilkinson [5],

$$\begin{gathered} A = 4, \quad B = 6, \quad C = 3, \quad D = 2, \quad E = 7, \quad F = 3, \\ A\&B = 2, \quad A\&F = 2, \quad B\&C = 2, \quad B\&D = 1, \\ B\&F = 2, \quad C\&D = 1, \quad D\&E = 1, \quad E\&F = 1, \\ A\&B\&F = 1, \quad \text{and} \quad B\&C\&D = 1, \end{gathered}$$

where we use the & operator as in Definition 2.1. We fit this specification with **venneuler** and **eulerr**, in the latter case using both circles and ellipses.

eulerr manages to fit this set configuration perfectly using ellipses (Section 3.1) and furthermore produces a better circular Euler diagram (Section 3.1) compared to **venneuler** (Section 3.1).

Micallef and Rodgers [3] features a diagram from Lenz and Fornoni [23] that they favorably remodelled using **eulerAPE**. We will do

[19] The specification of the computer was

- Microsoft Windows Pro 10 x64
- Intel® Core™ i7-4500U CPU @ 1.80GHz, 2 cores
- 8 GB memory

[20] This was a m4.large instance with the following specifications:

- Ubuntu 16.04 x64
- 2.4 GHz Intel Xeon®E5-2676 v3 (Broadwell) CPU, 2 cores
- 8 GB memory

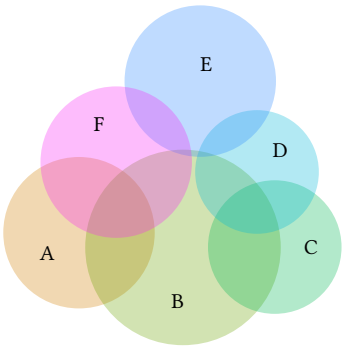

(a) The diagram from **venneuler**, with a stress of 0.007 and diagError of 0.013

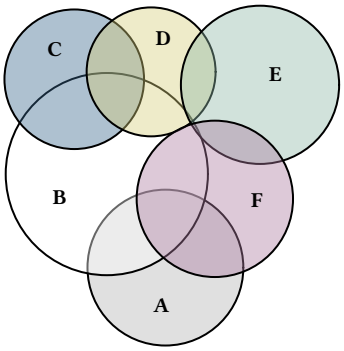

(b) The circular diagram from **eulerr**, with a stress of 0.004 and diagError of 0.011.

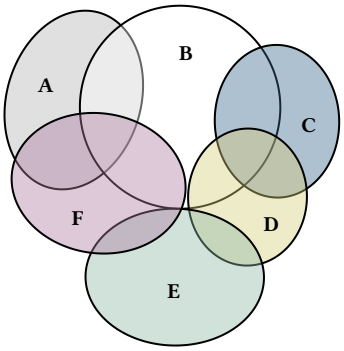

(c) The elliptical diagram from **eulerr**, with a stress of 2.587×10^{-13} and diagError of 9.944×10^{-8}.

Figure 3.1. A comparison of a Euler diagram generated with **venneuler** with two generated from **eulerr** with circles and ellipses respectively.

the same here, using **eulerr** and compare the results of the two packages. The data from the original diagram was

$$\begin{gathered} A = 0.36, \quad B = 0.03, \quad C = 0, \\ A\&B = 0.41, \quad A\&C = 0.04, \quad B\&C = 0, \quad \text{and} \\ A\&B\&C = 0.11. \end{gathered}$$

However, because **eulerAPE** cannot fit set configurations with empty intersections, the authors replaced 0 with 0.00001. Since the diagram was fitted with ellipses, we will do the same with **eulerr** but keep the areas as in the original data.

The fits from both packages are exact (Figure 3.2). Although we instructed **eulerr** to allow ellipses in the fit, the algorithm stuck to circles, which, given that the fit is exact, is the appropriate choice since circles are easier to interpret [7]. The reason **eulerAPE** did not is that it tries to keep the three shapes intersecting (albeit marginally), which cannot be done with circles if the layout is to be exact.

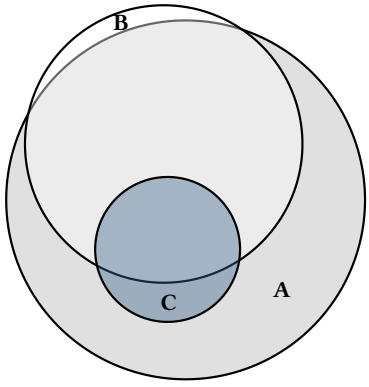

(a) The diagram from **eulerr**.

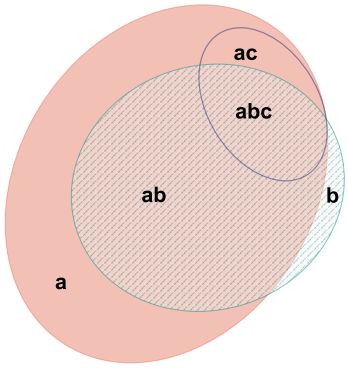

(b) The diagram from **eulerAPE**.

Figure 3.2. Diagrams from **eulerAPE** and **eulerr** based on data from a diagram in Lenz and Fornoni [23]. The diagram from **eulerAPE** has been modified to enlarge fonts and remove labels for *b* and *bc*, which had been added at seemingly arbitrary locations in the original diagram. Both diagrams are exact.

To conclude our case studies, we turn to a diagram that was featured on the website of the author of **venn.js** [24]. The diagram is based on the *Netflix Prize Dataset*[21], from which the author

	Amelie	Pulp Fiction	Miss Congeniality	Armageddon	Rashomon	Coyote Ugly
Amelie	38,753					
Pulp Fiction	15,197	70,153				
Miss Congeniality	1,829	3,854	37,837			
Armageddon	1,218	6,593	10,536	40,345		
Rashomon	2,087	2,799	132	143	6,209	
Coyote Ugly	610	2,206	5,965	5,699	38	15,611

Table 3.1. The data from the Netflix Prize dataset used by Frederickson [24].

> [...] picked 6 movies, kind of at random – and then represented them using the set of users that gave the movie a 5 star rating.

The movies were *Amelie, Pulp Fiction, Miss Congeniality, Armageddon, Rashomon,* and *Coyote Ugly*. The data only includes pairwise relationships (Table 3.1).

The fit from **eulerr** is marginally better than that of **venn.js**. The stress and diagError of the **eulerr** diagram (Figure 3.4a) are 0.003 and 0.014 respectively, whilst the same figures are 0.004 and 0.015 for the **venn.js** diagram (Figure 3.4b).

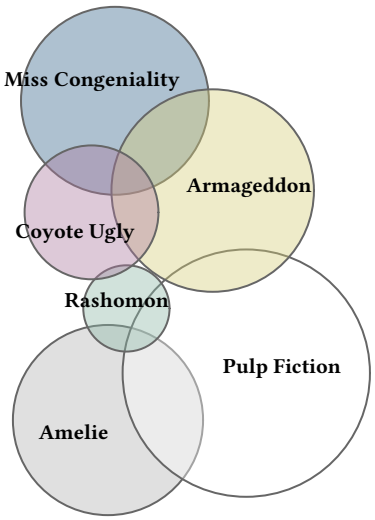

(a) The fit from **eulerr** with a stress of 0.003 and diagError of 0.014.

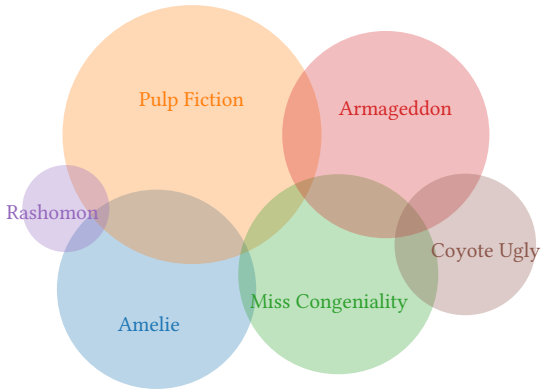

(b) The fit from **venn.js** with a stress of 0.004 and diagError of 0.015.

Figure 3.4. The Euler diagrams generated from the Netflix Prize data. The difference in the two layouts primarily concern the placements of *Rashomon* and *Miss Congeniality*.

3.2 Consistency

To compare the consistency among **eulerr**, **venneuler**, **eulerAPE**, **venn.js**, and **Vennerable**, we generate random diagrams of circles

and ellipses (separately), compute their areas, and attempt to reproduce the original diagrams using the various software. We restrict ourselves to diagrams consisting of between three and eight shapes.

For the circles, we sample radii (r_i) and coordinates (h_i and k_i) from

$$\begin{aligned} r_i &\sim \mathcal{U}(0.2, 0.6) \\ h_i, k_i &\sim \mathcal{U}(0, 1), \end{aligned} \tag{3.1}$$

where N is the number of shapes. For the ellipses, we sample semi-axes (a_i and b_i), coordinates (h_i and k_i), and rotation axes (ϕ_i) from

$$\begin{aligned} h_i, k_i &\sim \mathcal{U}(0, 1) \\ c_i &\sim \mathcal{U}(0.5, 2) \\ r_i &\sim \mathcal{U}(0.2, 0.6) \\ a_i &= c_i r_i \\ b_i &= \frac{r_i}{c_i} \\ \phi_i &\sim \mathcal{U}(0, \pi). \end{aligned} \tag{3.2}$$

Next, we compute the required areas, ω (Definition 2.1), for each iteration and fit a Euler diagram using the aforementioned packages. Finally, we compute and return *diagError* (2.7) and score each diagram as a success if its *diagError* is lower than 0.01, that is, if no portion of the diagram is 1% off (in absolute terms) from that of the input; note that this is always achievable since our input comes from sampled diagrams.

For each number of shapes ($N = 3, 4, \ldots, 8$) we run the simulations until we have achieved a 95% confidence interval around $\hat{p}$, the proportion of successful diagrams, that is no wider than 0. We use the normal approximation interval

$$\mathcal{I}(\hat{p})_{0.95} = \hat{p} \pm z_{0.95} \sqrt{\frac{\hat{p}(\hat{p} - 1)}{n}}.$$

The algorithm is formalized in Algorithm 1. For circular diagrams, **eulerr** outperforms **Vennerable** and **venneuler** in consistency by considerable margin and is on par with **venn.js** and **eulerAPE** (Figure 3.5). **eulerr** and **eulerAPE** are the only packages that successfully fits all of the circular diagrams (although **eulerAPE** only accepts a subset of our three-set diagrams). **venn.js** fails in 4 cases out of 6000.

For ellipses of three shapes, **eulerr** successfully fits all diagrams whilst **eulerAPE** fails in 6 cases out of 1000.

For ellipses of four or more sets—which only **eulerr** accepts—the consistency drops for each additional set, yet remains above 38%. **Vennerable**, which is only able to produce three-set diagrams, only produces accurate diagrams for 7% of the random layouts and moreover fails with an error in 6 cases.

for $N \leftarrow 3 : 8$ **do**
  $i \leftarrow 1$
  successes $\leftarrow 0$
  do
    $h_i, k_i \leftarrow \mathcal{U}(0, 1)$
    $r_i \leftarrow \mathcal{U}(0.2, 0.6)$
    if circle **then**
      $\omega_i \leftarrow$ FindOverlaps(h_i, k_i, r_i)
    else if ellipse **then**
      $c_i \leftarrow \mathcal{U}(0.5, 2)$
      $a_i \leftarrow c_i r_i$
      $b_i \leftarrow r_i / c_i$
      $\phi_i \leftarrow \mathcal{U}(0, \pi)$
      $\omega_i \leftarrow$ FindOverlaps$(h_i, k_i, a_i, b_i, \phi_i)$
    end if
    for all $j \leftarrow$ software packages **do**
      $\hat{p}_j \leftarrow$ successes$_j / i$
      $\Gamma(\hat{p}_j)_{0.95} \leftarrow 2 \times z_{0.95} \sqrt{\frac{\hat{p}_j(\hat{p}_j - 1)}{i}}$
      if $\Gamma(\hat{p}_j)_{0.95} > 0.02$ **or** $i < 1000$ **then**
        $A_{i_j} \leftarrow$ FitDiagram(ω_i)
        if DiagError$(A_{i_j}, \omega_i) < 0.01$ **then**
          successes$_j \leftarrow$ successes$_j + 1$
        end if
      end if
    end for
    $i \leftarrow i + 1$
  while all $\Gamma(\hat{p})_{0.95} > 0.02$ **or** $i < 1000$
end for

Algorithm 1. The algorithm used to simulate diagrams of circles or ellipses, reverse-engineer set relationships, and fit Euler diagrams to these relationships using the different software packages.

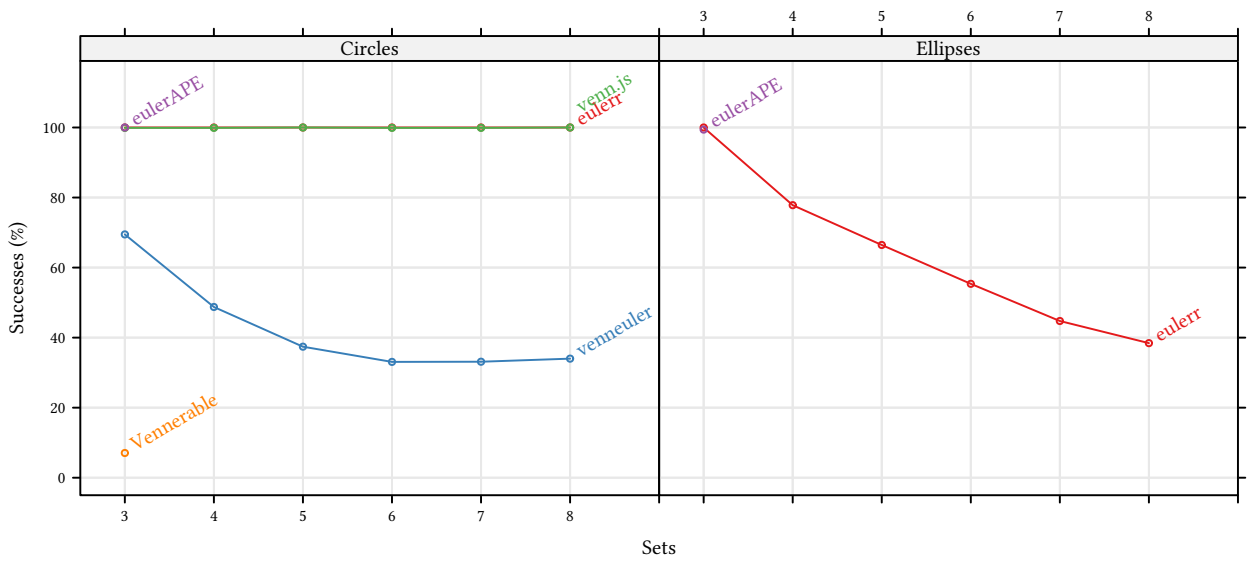

Figure 3.5. Proportions of successfully reproduced Euler diagrams from set configurations based on sampled circular and elliptical diagrams generated from the distributions in (3.1) and (3.2). The results are based on at least 1000 iterations for each software package and number of sets and have at most a 0.02-wide symmetric 0.95% confidence interval around the displayed point estimate. A success is defined as a diagram with a *diagError* (2.7) below 0.01.

3.3 Accuracy

In section 3.2, we assessed the efficacy in reproducing diagrams with exact, but unknown, solutions. Reality, however, often presents us with relationships that lack such exact solutions. Yet, when there is no exact solution, one might still exist that we deem *good enough*, which we naturally want our model to find.

To assess the proficiency of finding approximate solutions, we generate random set relationships that may or may not have exact solutions and fit Euler diagram using the software under study. For each $N = 3, 4, \ldots, 8$ sets and for a minimum of 1000 iterations, we initialize $2^N - 1$ permutations of set combinations, select one for each set, and initialize these to a number in $\mathcal{U}(\epsilon, 1)$, where ϵ is defined as the square root of the current machine's smallest representable difference between one and the smallest value greater than one[22]. After this, we pick 0 to $\binom{N-2}{1}$ elements from the $2^N - N - 1$ remaining permutations and assign to them a number from $\mathcal{U}(0, 1)$ as before.

[22] The relevant line of code used to generate this ϵ is `sqrt(.Machine$double.eps)`

As in section 3.2, we run our simulations until we achieve a 95% confidence interval around the mean diagError no wider than 0.02, but for a minimum of 1000 iterations. The confidence level we use is the based on the t-distribution:

$$\mathcal{I}(\bar{x})_{0.95} = \bar{x} \pm t_{0.95} \frac{S}{\sqrt{n}}, \tag{3.3}$$

where S is the sample standard deviation. he algorithm is formalized in Algorithm 2.

for $N \leftarrow 3 : 8$ **do**
  $i \leftarrow 1$
  $s \leftarrow 0$
  do
    $\omega_i = \{\omega_{i_1}, \omega_{i_2}, \ldots, \omega_{i_{2^N-1}}\} \leftarrow 0$
    for $3 : N$ **do**
      $k \leftarrow$ random index in $\{\omega_i : \omega_i \cap F_N \neq \emptyset\}$
      $\omega_{i_k} \leftarrow \mathcal{U}(\epsilon, 1)$
    end for
    $V \leftarrow$ random indices from $\{\omega_i : \omega_i = 0\}$
    $\{\omega_i : \omega_i = v\} \leftarrow \mathcal{U}(\epsilon, 1)$
    for all $j \leftarrow$ software packages **do**
      $A_{j_i} \leftarrow$ FitDiagram(ω_i)
      $x_{j_i} \leftarrow$ DiagError(A_{j_i}, ω_i)
      $s_j \leftarrow \sqrt{\frac{1}{i-1}\sum(x - \bar{x})^2}$
      $\Gamma(\bar{x}_j)_{0.95} \leftarrow 2 \times t_{0.95} s_j / \sqrt{i}$
    end for
    $i \leftarrow i + 1$
  while all $\Gamma(\bar{x})_{0.95} > 0.02$ **or** $i < 1000$
end for

Algorithm 2. The algorithm we use to simulate random set relationships and fit them with the software under study to assess their accuracy. $\Gamma(\bar{x})_{0.95}$ denotes a 95% confidence interval around the mean *diagError*, s is the corrected sample standard deviation, F is the collection of sets in the input, and ϵ is defined as the square root of the difference between 1 and the least value greater than 1 that is representable on our machine.

However, given that neither **Vennerable** nor **eulerAPE** are capable of fitting Euler diagrams that feature subset or disjoint relationships, and because fully intersecting diagrams are more difficult to fit—at least with circles—we run a separate treatment in which we modify Algorithm 2 so that every intersection is initialized to a value in $\mathcal{U}(\epsilon, 1)$.

From the results generated via Algorithm 2, we can surmise that elliptical **eulerr** diagrams achieve the lowest stress and diagError on average Figure 3.6. It is lower regardless of the number of sets, but is relatively more pronounced for sets of three and four shapes.

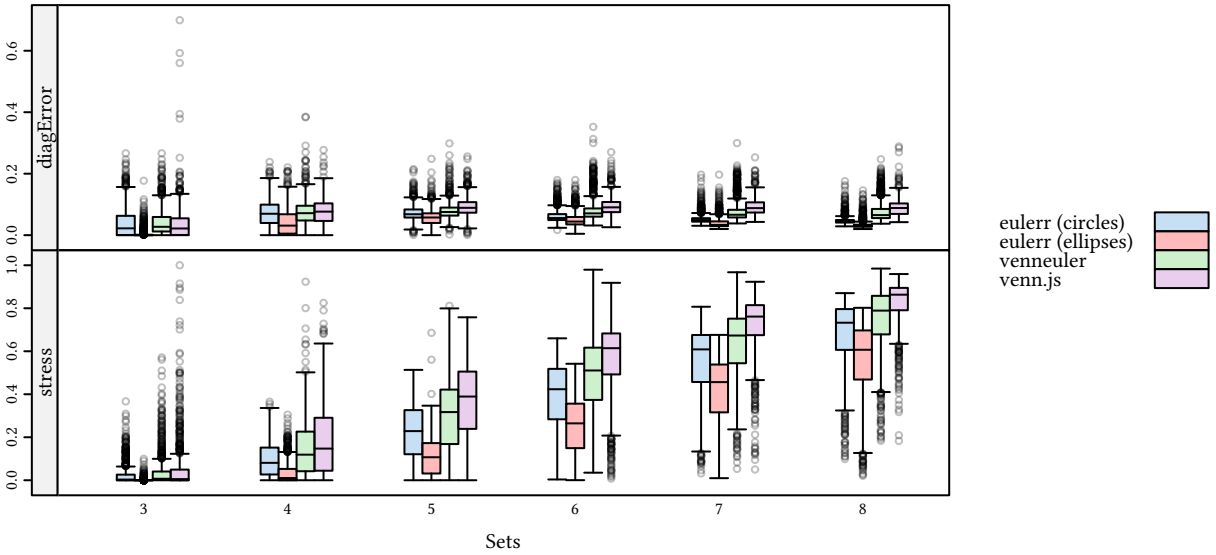

Figure 3.6. Tukey box plots of Euler diagrams based on set relationships that may or may not have perfect solutions, generated from (3.2).

We also find that among the algorithms that fit circular Euler diagrams, **eulerr** offers the lowest median stress across all the sizes of set relationships. For diagError, however, **venn.js** produces diagrams with the least loss for three sets, whilst **eulerr** scores better for all the remaining set sizes, for which **venn.js** is moreover outdone by **venneuler**.

Looking at the results from the simulation of three-set relationships with every intersection present (Figure 3.7), **eulerr** still produces the most accurate diagrams (provided that we use ellipses)—both in terms of stress and diagError. The difference next to **eulerAPE** is very small, however, with differences below 10^{-8}.

For the circular diagrams, **venn.js** achieves the lowest median diagError of 7.11×10^{-8} followed by **venneuler** at 8.219×10^{-7}, **eulerr** at 0.044, **eulerAPE** at 0.035, and **Vennerable** at 0.044. As for stress, however, the order is partially reversed with respective stress values at 4.581×10^{-14}, 7.834×10^{-12}, 0.022, 0.035, 0.044 for **eulerr**, **venneuler**, **venn.js**, **eulerAPE**, and **Vennerable** respectively.

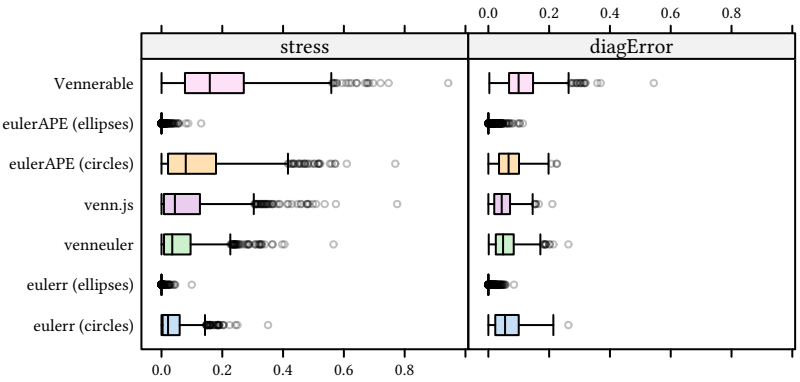

Figure 3.7. Tukey box plots of diagError and stress for Euler diagrams based on set relationships of three sets with every intersection present.

3.4 Performance

Using the same method as in section 3.3, we generate random set relationships and measure the time it takes for each software package to form a diagram from the fit. We rely on **microbenchmark** for the benchmarks, which randomizes the order in which the packages are called between trials. Because the current version of **venn.js** has not been implemented in R, nor any version of **eulerAPE**, we omit these packages from the performance benchmarks.

The violin plot in Figure 3.8 shows that **eulerr** is speedier for circular diagrams up to seven sets, at which point **venneuler** catches up and then surpasses the performance of **eulerr**. For a three set diagram, for instance, **eulerr** takes a median of 0.007 seconds to find a fit, whilst **venneuler** takes 0.414 seconds, and **Vennerable** 0.056 seconds. For eight sets, meanwhile, **eulerr** takes 2.68 seconds and **venneuler** 2.059.

The computation time for the elliptical diagrams from **eulerr** generally vary more but are still, on average, faster than **venneuler** for up to five sets—albeit with the exception of diagrams of three sets, where the resulting bimodal distribution is a consequence of the time-consuming last-ditch optimizer (subsection 2.3.3) that is activated by default if the fit is not error-free.

3.5 Availability

eulerr is available as an R package on the CRAN network [26] and is installed simply by typing

```
install.packages("eulerr")
```

A development version and the source code for the project is maintained in a GitHub repository at `https://github.com/jolars/eulerr`. This version can be installed, provided that the **devtools** package is installed, with the following oneliner:

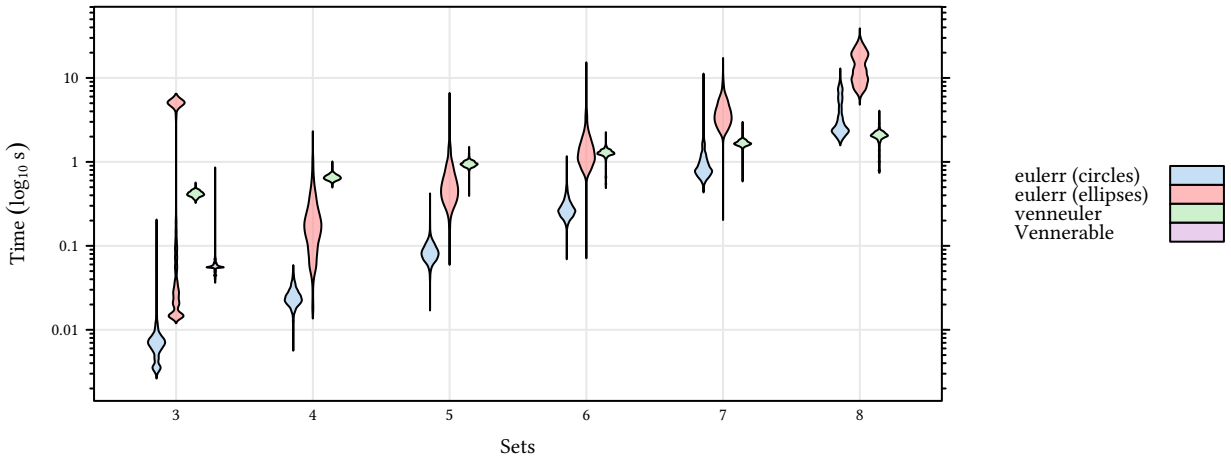

Figure 3.8. Violin plot of the performance of **eulerr**, **venneuler**, and **Vennerable** on random set relationships of three to eight sets. The density smoother is that of Sheather and Jones [25].

```
devtools::install_github("jolars/eulerr")
```

The source code for this thesis, meanwhile, is also provided in a GitHub repository at `https://github.com/jolars/eulerrPaper`, which also hosts the code used to generate the results for this thesis is provided.

Finally, there is a **shiny** [27] web application for **eulerr** at `http://jolars.co/eulerr`, which features a slightly slimmed-down version that only allows two types of input, offers less freedom in customizing the diagram, and does not feature the last-ditch optimizer. (See subsection 2.3.3). The web application s available to everyone with a internet connection and somewhat-recent web browser.

4 Discussion

In this paper, we have presented a novel method for generating Euler diagrams for any number of sets using ellipses. We have shown that the package performs better or on par with all the other packages for most of the analyses in this thesis. In addition, the method is speedier than the other R packages for set relationships with up to seven sets, wherafter it is eclipsed by **venneuler**.

eulerr reproduced all the circular diagrams generated in section 3.2 within our margin of error. No other package managed this task, although the failing diagrams of both **eulerAPE** and **venn.js** numbered in the single digits.

In contrast, **venneuler** was not (by our standards) able to adequately reproduce between 30 and 65% of these diagrams, which, however, was still better than the results on a previous test2 [28]. Some of these diagrams feature disjoint or subset relationships, which **venneuler** have problems fitting on account of its initial optimizer. As we discussed in chapter 1, **eulerr**, **venn.js**, and **venneuler** all use multi-dimensional scaling for their initial diagram. **venneuler**, however, unnecessarily restricts the locations of disjoint and subset circles. Given, for instance, two disjoint sets, the algorithm will attempt to place them tangent to one another; otherwise, the optimizer will report loss. Likewise, for a subset relationship, **venneuler** tries to place the smaller circle at the exact midpoint of the enclosing shape.

For the fit to be accurate, however, those restrictions are pointless as long as the sets remain disjoint or subset and almost always feature other locations that fulfill those requirements. For **venneuler**, this becomes problematic when the required positions interfere with locations of other sets that need to use that space. The MDS algorithm from **venn.js** and **eulerr** circumvents this by assigning a loss and gradient of zero when the pairwise set intersection *and* the candidate circles are disjoint or subset. This makes it easier for the starting layout to find a good initial layout.

Another reason for the mediocre results of **venneuler** could be both that the optimizer terminates prematurely in case the relative reduction in stress is considered negligible between iterations *or* that the number of iterations is generally too low.

eulerr managed to also reproduce all of the elliptical three-set diagrams perfectly but failed for a considerable portion as the number of sets in the input surged. For three-set diagrams, **eulerr** employs a rigorous last-ditch optimizer in case the fit it not adequate[23] after

[23] Here, we define *adequate* as a diagram with diagError below 0.001.

the "final" optimization step. This step is time-consuming (as we saw in section 3.4), but if activated would yield better results also for sets of more than three shapes.

The elliptical diagrams from **eulerr** are more accuracte for random set relationships (that might lack exact solutions) than all the other packages in this thesis, although the elliptical diagrams from **eulerAPE** were almost as accurate. Elliptical Euler diagrams are more successful since they, as we briefly covered in chapter 1, allow two addition degrees of freedom for each set. The gain is greatest for three sets and shrinks as we add more sets. This is what we expect: complicated inputs require complicated models and there are many diagrams that even elliptical Euler diagrams cannot fit—consider, for instance, the complicated geometry of the Venn diagram in Figure 4.1 that is required to represent all the intersections between six sets.

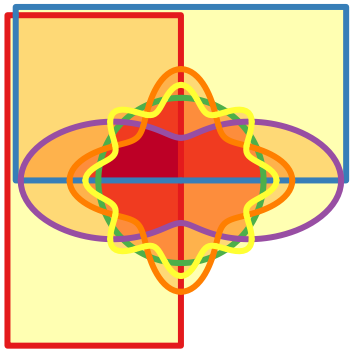

Figure 4.1. A six-set Venn diagram using Edward's method [29]; this diagram was generated with **Vennerable**.

Considering only circular Euler diagrams, **eulerr** remains the best choice for both diagError and stress in all cases except for three-set diagrams, where it ranks best in terms of stress but not diagError[24]; **venn.js** scores lowest. Interestingly—as well as surprisingly, given the results from section 3.2—**venn.js** performs worse than **venneuler** in all of the remaining cases. We can only speculate as to reasons for this, but it possible that the Nelder–Mead variant that was written for **venn.js** has trouble finding a good fit; indeed, this was our experience when designing **eulerr**, which at one point featured a variety of the same optimizer; in our case, `nlm()` from R, which uses numerical derivatives, was found to be superior.

For three to seven sets, **eulerr** is faster than both **Vennerable** and **venneuler**. The reason for this is partly the implementation in C++ and the use of the Armadillo library [30] provided by the interfaces **Rcpp** [31] and **RcppArmadillo** [32]. The second reason is the exact-area computations that outperform the quadtree binning of **venneuler** for the lower amount of sets. Paradoxically, this is also why the performance of **eulerr** suffers as the number of sets increase beyond seven.

The bottleneck in **eulerr**'s performance is the final optimization. It has to examine every possible intersection when computing the areas. For eight sets, for instance, this means investigating 255 intersections. In theory, the algorithm should converge in $O(2^n)$ time. Wilkinson [5], meanwhile, report convergence in $O(n)$ time. There is evidence of this in Figure 3.8 and it is possible that a fine-tuned version of **venneuler**'s algorithm might outperform **eulerr** also for lower number of sets. Regardless, the increasing computational demand of large number of sets make fitting such diagrams prohibitive at least in exploratory data analysis. Although it is questionable whether there is much use for Euler diagrams for such complicated diagrams—only rarely willl they surrender to an adequate fit—future versions of this algorithm should consider implementing approximate area-calculations when the number of sets

[24] It might be appropriate to note that **eulerr** and **venn.js** both attempt to minimize the sums of squares and not diagError.

is large.

Fitting diagrams is substantially harder with ellipses than with circles. There are many more local minimi that might hobble our optimizer and since our initial configuration only considers circles, such minimi cannot reliably be avoided before the final optimization step. And because we moreover default to a semi-local optimizer in this final step, it is not uncommon that we become stuck before finding the global minimum. The last-ditch optimizer battles such minimi with brute force: it tries a considerable number of permutations and uses the previous fits (initial and semi-final) only to set up constraints for the algorithm. The downside to using this optimizer is that it, in contrast to us, people[25], does not prefer circles over ellipses, which means that we might get diagrams with ellipses when circles would do just as well.

[25] And the other optimizer that begins with an initial layout of circles.

4.1 Conclusion

In the majority of scenarios examined in this thesis, **eulerr** offers solutions with the least error among all of the packages tested. For three sets, its performance is equalled by the elliptical diagrams that **eulerAPE** produce, which, however, impose the restrictions that **eulerr** do not, namely, that there be no disjoint or subset relationships. In addition, **eulerr** offers considerable control over the visual output, which is levied via the **lattice** package for R.

eulerAPE's restriction to three sets is discussed by the authors of the package, who motivate this limitation with the propensity of Euler diagrams with more sets to lack adequate solutions and that their complexity make implementations difficult [9]. Whilst it is true that inputs with more than three sets do not always reduce to adequate Euler diagrams, it is our stance that those that do warrant a software implementation that can help the user find them, given that Euler diagrams are intuitive graphics that are appreciated by most viewers.

The primary shortcoming of **eulerr** lies in its failure to consistently reproduce random elliptical diagrams (see section 3.2), implying that the performance in producing random set relationships (see section 3.3) must have potential to improve. This is not an intractable problem and we argue that it can be overcome either by

- relying on brute force global optimizers that thoroughly examine the search space and attempt to optimize, and possibly parallelize, these to make larger diagrams fit within a reasonable time span, or
- designing an algorithm for the initial configuration that works specifically for ellipses.

Whichever direction future algorithms take, we believe that the advances presented in this thesis should serve as another step forward towards more accurate Euler diagrams.

4.2 Acknowledgements

Thanks to blabla.

Appendices

A Visualization

Once we have ascertained that our Euler diagram fits well, we can turn to visualizing the solution. For this purpose, **eulerr** leverages the **Lattice** graphics system [33] for R to offer intuitive and granular control over the output.

Plotting the ellipses is straightforward using the parametrization of a rotated ellipse,

$$\begin{bmatrix} x \\ y \end{bmatrix} = \begin{bmatrix} h + a\cos\theta \\ k + b\sin\theta \end{bmatrix}, \quad \text{where } \theta \in [0, 2\pi].$$

Often, however, we would also like to label the ellipses and their intersections with text and this is considerably more involved.

A.1 Labeling

Labeling the ellipses is difficult because the shapes of the intersections often are irregular, lacking a well-defined center; we know of no analytical solution to this problem. As usual, however, the next-best option turns out to be a numerical one. First, we locate a point that is inside the required region by spreading points across the discs involved in the set intersection. To distribute the points, we use a modification of *Vogel's method* [34, 35] adapted to ellipses. Vogel's method spreads points across a disc using

$$p_k = \begin{bmatrix} \rho_k \\ \theta_k \end{bmatrix} = \begin{bmatrix} r\sqrt{\frac{k}{n}} \\ \pi(3 - \sqrt{5})(k-1) \end{bmatrix} \quad \text{for } k = 1, 2, \ldots, n. \tag{A.1}$$

In our modification, we scale, rotate, and translate the points formed in (A.1) to match the candidate ellipse. We rely, as before, on projective geometry to carry out the transformations in one go:

$$p' = \begin{bmatrix} x' \\ y' \\ 1 \end{bmatrix} = \begin{bmatrix} 1 & 0 & h \\ 0 & 1 & k \\ 0 & 0 & 1 \end{bmatrix} \begin{bmatrix} \cos\phi & \sin\phi & 0 \\ -\sin\phi & \cos\phi & 0 \\ 0 & 0 & 1 \end{bmatrix} \begin{bmatrix} a & 0 & 0 \\ 0 & b & 0 \\ 0 & 0 & 1 \end{bmatrix} \begin{bmatrix} \hat{x} \\ \hat{y} \\ 1 \end{bmatrix}$$

After we spread our points throughout the ellipse and find a point, p_i', that is contained in our desired intersection, we proceed to optimize its position numerically. The position we are looking for is that which maximizes the distance to the closest ellipse in our diagram to provide as much margin as possible for the label. This is a maximin problem with a loss function equal to

$$\max_{x,y \in \mathbb{R}^2} \min_{i=1,2,\ldots,N} f(x, y, h_i, k_i, a_i, b_i, \phi_i) \tag{A.2}$$

where f is the function that determines the distance from a point (x, y) to the ellipse defined by h, k, a, b and ϕ.

Similarly to fitting Euler diagrams in the general case, there appears to be no analytical solution to computing the distance from a point to an ellipse. The numerical solution we use has been described in Eberly [36] and involves solving the roots to a quartic polynomial via a robust bisection optimizer.

To optimize the location of the label, we employ a version of the *Nelder–Mead Method* [37] which has been translated from Kelley [38] and adapted for **eulerr** to ensure that is coverges quickly and that the simplex remains within the intersection boundaries (since we want the local maximum). The method is visualized in Figure A.1.

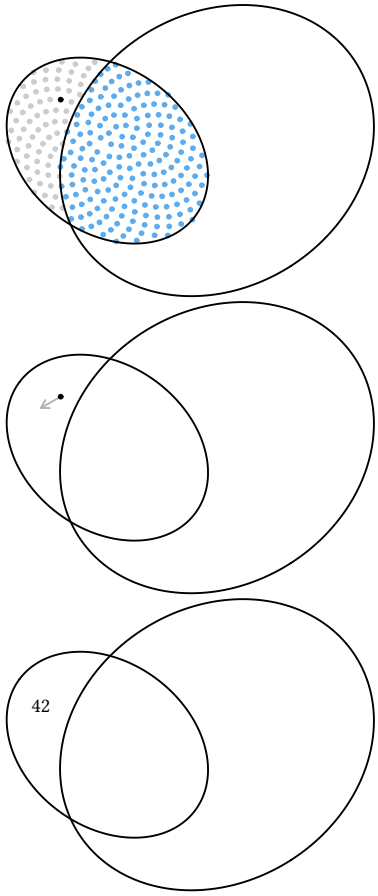

Figure A.1. The method eulerr uses to locate an optimal position for a label in three steps from top to bottom: first, we spread sample points on one of the ellipses and pick one inside the intersection of interest, then we begin moving it numerically, and finally place our label.

A.2 Aesthetics

Euler diagrams display both quantitative and qualitative data. The quantitative aspect is the quantities or sizes of the sets depicted in the diagram and is visualized by the relative sizes, and possibly the labels, of the areas of the shapes—this is the main focus of this paper. The qualitative aspects, meanwhile, consist of the mapping of each set to some quality or category, such as having a certain gene or not. In the diagram, these qualities can be separated through any of the following aesthetics:

- color,
- border type,
- text labelling,
- transperancy,
- patterns,

or a combination of these. The main purpose of these aethetics is to separate out the different ellipses so that the audience may interpret the diagram with ease and clarity.

Among these aesthetics, the best choice (from a viewer perspective) appears to be color [7], which provides useful information without extraneous chart junk [39]. The issue with color, however, is that it cannot be perceived perfectly by all—8% of men and 0.4% of women in European Caucasian countries, for instance, suffer the most common form, red–green color deficiency [40]. Moreover, color is often printed at a premium in scientific publications and adds no information to a diagram of two shapes.

For these reasons, **eulerr** defaults to distinguishing ellipses with color using a color palette generated via the R package **qualpalr** [41], which automatically generates qualitative color palettes based on a perceptual model of color vision that optionally caters to color

vision deficiency. This palette has been manually modified to fullfil our other objectives of avoiding using colors for two sets. The first eight colors of the pallete are visualized in Figure A.2.

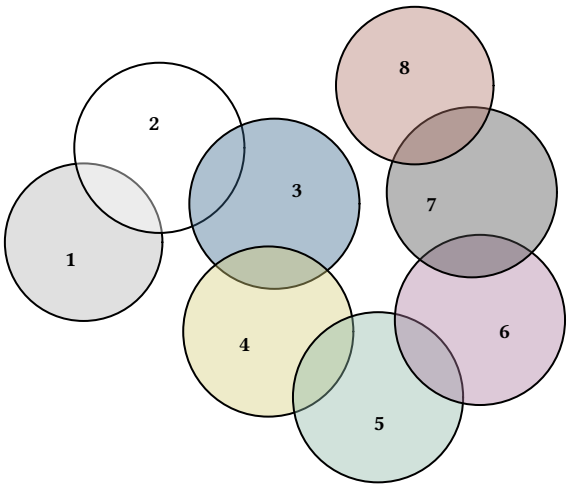

Figure A.2. The eight first colors of the default color palette.

A.3 Normalizing dispered layouts

If there are disjoint clusters of ellipses, the optimizer will often spread these out more than is necessary, wasting space in our diagram. To tackle this, we use a SKYLINE-BL rectangle packing algorithm [42] designed specifically for **eulerr**. In it, we surround each ellipse cluster with a bounding box, pack these boxes into a bin of appropriate size and aspect ratio, and adjust the coordinates of the ellipses in the clusters to compact our diagram.

As a bonus, this also increases the chance of having similar layouts for different function calls even when we do not fix the random seed.

B Usage

`euler()` and `plot()` are the only functions that a user of **eulerr** need concern themselves with. In section 2.1, we described the various forms of input that the function can be supplied with. Using the first form, we will showcases how a Euler diagram is fit. For this example, we use a diagram from a publication by Junta et al. [43] that was also showcased in Wilkinson [5]. We load the package, specify our diagram, and fit it using `euler()` as follows.

```
library(eulerr)
junta_2009 <- c("SE" = 13, "Treat" = 28, "Anti-CCP" = 101,
                "DAS28" = 91, "SE&Treat" = 1, "SE&DAS28" = 14,
                "Treat&Anti-CCP" = 6, "SE&Anti-CCP&DAS28" = 1)
fit1 <- euler(junta_2009)
```

Printing the results provides a summary of the fit, including the *stress* and *diagError* metrics that were introduced in section 2.4.

```
fit1 # or equivalently print(fit1)


##                          original fitted residuals regionError
## SE                             13 12.780     0.220       0.000
## Treat                          28 27.525     0.475       0.000
## Anti-CCP                      101 99.287     1.713       0.002
## DAS28                          91 89.457     1.543       0.001
## SE&Treat                        1  0.983     0.017       0.000
## SE&Anti-CCP                     0  0.000     0.000       0.000
## SE&DAS28                       14 13.763     0.237       0.000
## Treat&Anti-CCP                  6  5.898     0.102       0.000
## Treat&DAS28                     0  0.000     0.000       0.000
## Anti-CCP&DAS28                  0  0.000     0.000       0.000
## SE&Treat&Anti-CCP               0  0.000     0.000       0.000
## SE&Treat&DAS28                  0  0.000     0.000       0.000
## SE&Anti-CCP&DAS28               1  0.000     1.000       0.004
## Treat&Anti-CCP&DAS28            0  0.000     0.000       0.000
## SE&Treat&Anti-CCP&DAS28         0  0.000     0.000       0.000
##
## diagError: 0.004
## stress:    0
```

The fit is more or less equivalent to that of **venneuler** [5]. There *is* an error but it is small at a diagError of 0.004. We could, however, try to improve the fit using ellipses:

```
# Fit the data using ellipses instead
fit2 <- euler(junta_2009, shape = "ellipse")

# Compare the fits on diagerror
fit1$diagError - fit2$diagError


## [1] 0
```

Comparing the two fits in diagError, however, shows that we have not bettered the fit in any meaningful way. Our next goal is to visualize the layout, which we do both using the default options and by customizing the fit, adding quantities, replacing the sets' labels with a key, removing lines, and changing the fills using the **RColorBrewer** package (Figure B.1).

```
p1 <- plot(fit1)
p2 <- plot(fit1,
           quantities = list(fontface = 3),
           fill = RColorBrewer::brewer.pal(4, "Set2"),
           border = "transparent",
           auto.key = list(space = "right")) # key on the right
```

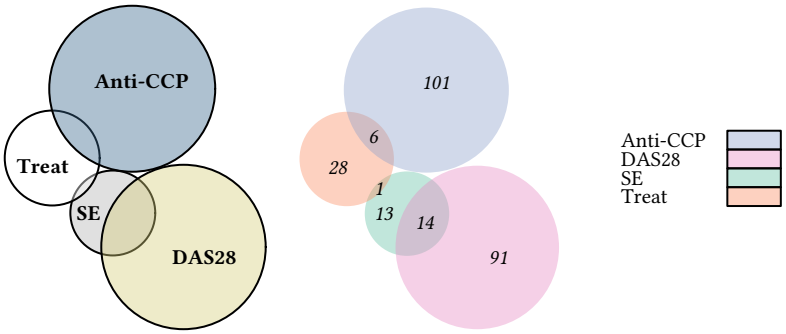

(a) The default settings.

(b) Custom plot settings.

Figure B.1. The same fit visualized in two distinct ways.

Bibliography

[1] Leonhard Euler. *Letters of Euler to a German princess, on different subjects in physics and philosophy.* Murray and Highley, 1802. URL http://archive.org/details/letterseulertoa00eulegoog.

[2] Jonathan Swinton. *Vennerable: Venn and Euler area-proportional diagrams*, 2011. URL https://github.com/js229/Vennerable. R package version 3.1.0.9000.

[3] Luana Micallef and Peter Rodgers. eulerAPE: drawing area-proportional 3-Venn diagrams using ellipses. *PLOS ONE*, 9(7):e101717, July 2014. ISSN 1932-6203. doi: 10.1371/journal.pone.0101717.

[4] Luana Micallef and Peter Rodgers. eulerForce: force-directed layout for Euler diagrams. *Journal of Visual Languages and Computing*, 25(6): 924–934, December 2014. ISSN 1045-926X. doi: 10.1016/j.jvlc.2014.09.002.

[5] L. Wilkinson. Exact and approximate area-proportional circular Venn and Euler diagrams. *IEEE Transactions on Visualization and Computer Graphics*, 18(2):321–331, February 2012. ISSN 1077-2626. doi: 10.1109/TVCG.2011.56.

[6] Hans A. Kestler, André Müller, Johann M. Kraus, Malte Buchholz, Thomas M. Gress, Hongfang Liu, David W. Kane, Barry R. Zeeberg, and John N. Weinstein. VennMaster: area-proportional Euler diagrams for functional GO analysis of microarrays. *BMC Bioinformatics*, 9:67, January 2008. ISSN 1471-2105. doi: 10.1186/1471-2105-9-67.

[7] Andrew Blake. *The impact of graphical choices on the perception of Euler diagrams.* Ph.D. dissertation, Brighton University, Brighton, UK, February 2016. URL http://eprints.brighton.ac.uk/15754/1/main.pdf.

[8] Stirling Christopher Chow. *Generating and drawing area-proportional Euler and Venn diagrams.* Ph.D. dissertation, University of Victoria, Victoria, BC, Canada, 2007. URL http://citeseerx.ist.psu.edu/viewdoc/download?doi=10.1.1.126.2678&rep=rep1&type=pdf.

[9] Luana Micallef. *Visualizing set relations and cardinalities using Venn and Euler diagrams.* Ph.D. dissertation, University of Kent, September 2013. URL https://kar.kent.ac.uk/47958/.

[10] Ben Frederickson. venn.js: area proportional Venn and Euler diagrams in JavaScript, November 2016. URL https://github.com/benfred/venn.js. original-date: 2013-05-09T17:13:20Z.

[11] David Eberly. The area of intersecting ellipses, November 2016. URL https://www.geometrictools.com/Documentation/AreaIntersectingEllipses.pdf.

[12] Jürgen Richter-Gebert. *Perspectives on Projective Geometry: A Guided Tour Through Real and Complex Geometry.* Springer, Berlin, Germany, 1 edition, February 2011. ISBN 978-3-642-17286-1.

[13] Stirling Chow and Peter Rodgers. Constructing area-proportional Venn and Euler diagrams with three circles. In *Euler Diagrams Workshop 2005*, pages 182–196, August 2005. URL http://www.cs.kent.ac.uk/pubs/2005/2354.

[14] Ben Frederickson. A better algorithm for area proportional venn and euler diagrams, June 2015. URL http://www.benfrederickson.com/better-venn-diagrams/.

[15] Robert B. Schnabel, John E. Koonatz, and Barry E. Weiss. A modular system of algorithms for unconstrained minimization. *ACM Trans Math Softw*, 11 (4):419–440, December 1985. ISSN 0098-3500. doi: 10.1145/6187.6192.

[16] R Core Team. *R: A Language and Environment for Statistical Computing.* R Foundation for Statistical Computing, Vienna, Austria, 2017. URL https://www.R-project.org/.

[17] John C. Nash. *Nonlinear parameter optimization using R tools.* Wiley, Chichester, West Sussex, 1 edition edition, May 2014. ISBN 978-1-118-56928-3.

[18] Darel R. Finley. Ultra-easy algorithm with C code sample. http://alienryderflex.com/polygon_area/, December 2006. URL http://alienryderflex.com/polygon_area/.

[19] Dirk Eddelbuettel. *RcppDE: Global Optimization by Differential Evolution in C++*, 2016. URL https://CRAN.R-project.org/package=RcppDE. R package version 0.1.5.

[20] Katherine M. Mullen, David Ardia, David L. Gil, Donald Windover, and James Cline. DEoptim: An R package for global optimization by differential Evolution. *Journal of Statistical Software*, 40(6), April 2011. doi: 10.18637/jss.v040.i06. URL https://www.jstatsoft.org/article/view/v040i06.

[21] Yang Xiang, Sylvain Gubian, Brian Suomela, and Julia Hoeng. Generalized simulated annealing for global optimization: the GenSA package. *The R Journal*, 5(1):13–28, June 2013. URL https://journal.r-project.org/archive/2013/RJ-2013-002/index.html.

[22] Jeroen Ooms. *V8: Embedded JavaScript Engine for R*, 2017. URL https://CRAN.R-project.org/package=V8. R package version 1.5.

[23] Oliver Lenz and Alessia Fornoni. Chronic kidney disease care delivered by US family medicine and internal medicine trainees: results from an online survey. *BMC medicine*, 4:30, December 2006. ISSN 1741-7015. doi: 10.1186/1741-7015-4-30.

[24] Ben Frederickson. Venn diagrams with D3.js, June 2015. URL http://www.benfrederickson.com/venn-diagrams-with-d3.js/.

[25] Simon Sheather and M. C. Jones. A Reliable Data-Based Bandwidth Selection Method for Kernel Density Estimation. *Journal of the Royal Statistical Society*, 53(3):683–690, January 1991. doi: 10.2307/2345597. DOI: 10.2307/2345597.

[26] R Core Team. The Comprehensive R Archive Network, November 2017. URL https://CRAN.R-project.org/.

[27] Winston Chang, Joe Cheng, JJ Allaire, Yihui Xie, and Jonathan McPherson. *shiny: Web Application Framework for R*, 2017. URL https://CRAN.R-project.org/package=shiny. R package version 1.0.5.

[28] Ben Frederickson. venn.js compared to venneuler, June 2015. URL http://benfred.github.io/venn.js/tests/venneuler_comparison/.

[29] A. W. F. Edwards. *Cogwheels of the Mind: The Story of Venn Diagrams*. Johns Hopkins University Press, Baltimore, USA, 1 edition, April 2014. ISBN 978-0-8018-7434-5. URL https://jhupbooks.press.jhu.edu/content/cogwheels-mind.

[30] Conrad Sanderson and Ryan Curtin. Armadillo: a template-based C++ library for linear algebra. *The Journal of Open Source Software*, 1(2): 26, 2016. doi: 10.21105/joss.00026. URL http://joss.theoj.org/papers/10.21105/joss.00026.

[31] Dirk Eddelbuettel and Romain François. Rcpp: Seamless R and C++ integration. *Journal of Statistical Software*, 40(8):1–18, 2011. URL http://www.jstatsoft.org/v40/i08/.

[32] Dirk Eddelbuettel and Conrad Sanderson. RcppArmadillo: accelerating R with high-performance C++ linear algebra. *Computational Statistics and Data Analysis*, 71:1054–1063, March 2014. doi: 10.1016/j.csda.2013.02.005.

[33] Deepayan Sarkar. *Lattice: multivariate data visualization with R*. Use R! Springer, New York, USA, 2008. ISBN 978-0-387-75968-5. URL http://www.springer.com/us/book/9780387759685.

[34] Mary K. Arthur. Point picking and distributing on the disc the sphere. Final ARL-TR-7333, US Army Research Laboratory, Weapons and Materials Research Directorate, Abedeen, USA, July 2015. URL www.dtic.mil/get-tr-doc/pdf?AD=ADA626479.

[35] H. Vogel. A better way to construct the sunflower head. *Mathematical Biosciences*, 44(3-4):179–189, 1979. doi: 10.1016/0025-5564(79)90080-4.

[36] Eberly. Distance from a point to an ellipse, an ellipsoid, or a hyperellipsoid, November 2016. URL https://www.geometrictools.com/Documentation/DistancePointEllipseEllipsoid.pdf.

[37] J. A. Nelder and R. Mead. A simplex method for function minimization. *The Computer Journal*, 7 (4):308–313, January 1965. ISSN 0010-4620. doi: 10.1093/comjnl/7.4.308. URL https://academic.oup.com/comjnl/article/7/4/308/354237/A-Simplex-Method-for-Function-Minimization.

[38] C. T. Kelley. *Iterative methods for optimization*. Number 18 in Frontiers in applied mathematics. Society for Industrial and Applied Mathematics, Philadelphia, USA, 1 edition edition, 1999. ISBN 0-89871-433-8.

[39] Edward R. Tufte. *The visual display of quantitative information*. Graphics Press, Cheshire, CT, USA, 2 edition, May 2001. ISBN 978-1-930824-13-3.

[40] Jennifer Birch. Worldwide prevalence of red-green color deficiency. *Journal of the Optical Society of America. A, Optics, Image Science, and Vision*, 29(3): 313–320, March 2012. ISSN 1520-8532.

[41] Johan Larsson. *qualpalr: Automatic Generation of Qualitative Color Palettes*, 2016. URL https://cran.r-project.org/package=qualpalr. R package version 0.3.1.

[42] Jukka Jylänki. A thousand ways to pack the bin – a practical approach to two-dimensional rectangle bin packing, February 2010. URL http://clb.demon.fi/files/RectangleBinPack.pdf.

[43] Cristina Moraes Junta, Paula Sandrin-Garcia, Ana Lúcia Fachin-Saltoratto, Stephano Spanó Mello, Renê D. R. Oliveira, Diane Meyre Rassi, Silvana Giuliatti, Elza Tiemi Sakamoto-Hojo, Paulo Louzada-Junior, Eduardo Antonio Donadi, and Geraldo A. S. Passos. Differential gene expression of peripheral blood mononuclear cells from rheumatoid arthritis patients may discriminate immunogenetic, pathogenic and treatment features. *Immunology*, 127(3):365–372, July 2009. ISSN 1365-2567. doi: 10.1111/j.1365-2567.2008.03005.x.